



## ENVIRONMENTAL DISTURBANCE MODELS FOR SATELLITES, EDM

**Valdemir Carrara**

valdemir.carrara@inpe.br

Instituto Nacional de Pesquisas Espaciais, INPE

Av. dos Astronautas, 1758. Jd da Granja, São José dos Campos, SP, Brasil

**Abstract.** *This paper presents the design and development of a C++ library to compute the main disturbances on orbit and attitude of low Earth orbit satellites. The mathematical models as well the way the EDM (Environmental Disturbance Models) library can be operated and used as will also be shown. The EDM library has functions to calculate the forces and torques acting on satellites due to the space environment, which modify both the satellite orbit and attitude. The forces can then be used in a numerical integrator for accurate orbit computation, while the torque can also be integrated to obtain the attitude motion. The main effects included in the EDM are: aerodynamic and solar radiation pressure forces and torques, magnetic and gravity gradient torques, and accelerations due to the Earth, Sun and Moon gravitational fields. The models for the calculation of aerodynamic effects and solar radiation pressure require knowledge of the satellite geometry. This geometry can be described by means of function calling to define triangles or quadrilaterals which forms the satellite outer surface, or alternatively can also be provided by a geometry description file with Nastran commands. Some examples of forces and torques computation on simple geometries will be shown. Two other examples based on satellite CBERS (China Brazil Earth Remote Sensing Satellite) will be presented: the center of pressure position as function of the solar radiation incidence on the satellite and a comparison between the observed orbit decay and a numerically propagated orbit.*

**Keywords:** *Orbit disturbances, Attitude disturbances, Artificial satellites, Aerodynamic drag, Solar radiation pressure*

## 1 INTRODUCTION

The high-precision instruments used nowadays to determine both the position and orientation of artificial satellites, like GPS receivers and star trackers, requires that the dynamic models of the orbit and attitude have compatible accuracy. Because of this fact, several empirical models had successive enhancements to take account not only for better precision requirements, but especially due to the availability of new observational data stemmed from scientific satellites, that generated new models of the Earth's gravitational field, properties of the upper atmosphere, space weather and geomagnetic field. In this paper a library for numerical computation of perturbations in the orbit and attitude of artificial earth satellites is presented, which incorporates the latest models of the space environment and models for accurate calculation of major disturbances in low satellite orbits. This library currently consists of modules to compute the aerodynamic and solar radiation forces and torques (up to 1200 km altitude), magnetic and gravity gradient torques, and the geo-potential and sun-moon accelerations. Together, these forces and torques allow numerical integration of both orbit and attitude with the required accuracy. The library was fully developed in C++, but can be easily linked to programs written in other languages like Fortran or Visual Basic. The modules follow standardized procedures already adopted in a previously developed attitude simulation package, so they are totally compatible. The models adopted for the aerodynamic torques and solar radiation pressure depend on the satellite geometry. Several functions were implemented in order to compute the forces and torques on simply geometries such as spheres, cylinders and parallelepipeds (boxes) or any composition of these ones. For non Euclidian geometries there are functions that allow the satellite to be described by a finite set of flat elements, whose elemental forces can then be integrated in the outer area exposed to the aerodynamic flow or solar radiation. There is also the possibility to describe the surface of the satellite through a Nastran-type file, which can be created by any graphic editing program geometry, and thereafter converted to Nastran. The aerodynamic effects were modeled according to the Maxwell's kinetic theory of rarefied gases that uses the normal and tangential momentum accommodation coefficients. The radiation pressure model takes into account the specular reflection, diffuse and emissivity of each surface element of the satellite. To compute the geomagnetic field it was adopted the IGRF10 model, coded originally in Fortran and converted to C. Several models of the upper atmosphere properties were included in the package and they can be individually selected. The position of the Sun and Moon are obtained with 1 arc minute accuracy from the model based on *Astronomical Almanac 1987*.

This library was developed with the purpose to be used in an attitude and orbit simulator package. The simulator itself will be employed in a future environment aimed for developing embedded three axes attitude control systems that will equip upcoming Brazilian space missions. The degree of realism of the models ensures good fidelity and excellent representation of the physical phenomenon, to assure the required reliability of the control system and to make it work properly in the space environment. The intention of this paper is therefore to present the design of the EDM (Environmental Disturbance Models) library, its basic mathematical models and the way it can be operated and used. Some results coming from application examples will be shown, based on satellite CBERS (China Brazil Earth Remote Sensing Satellite), including a comparison between the observed orbit decay and a numerically computed orbit with the disturbance forces detailed in this work.

The modeling of the environmental disturbance effects is presented in next section. Section 3 describes the EDM library and the geometry data file. Some application examples

are shown in Section 4, together with the results of those examples. Finally, conclusions are presented in Section 5.

## 2 ENVIRONMENTAL PERTURBATION MODELS

A precise orbit determination algorithm relies always on the orbit dynamics, which, in turn, depends on how accurate is the orbit perturbation model. There are several sources of orbit and attitude perturbations in the space environment acting from low to high altitude orbits and also in the interplanetary ones. They can be grouped in gravitational, electromagnetic and surface interaction sources, with intensities extending from  $10^{-3}$  N (it depends on the spacecraft size, actually) down to  $10^{-30}$  N and beyond. Of course, such a small magnitude sources can be detected only in satellites with particular shapes where all the major effects are cancelled or simply not applicable for that orbit. For low Earth orbit where most satellites are, the main perturbation is the drag or aerodynamic force, followed by the solar radiation pressure, if one does not take into account the orbit distortion due to the non-uniformity of the Earth's gravitational field. Gravity gradient torque plays an important role in asymmetric satellites, but only in attitude. Also a source of torques is the interaction of the magnetic field of the satellite generated by unbalanced electrical currents or by the on-board magnetic materials with the Earth's magnetic field. Finally, mutual interaction between an electrically conducting satellite with the ionosphere and the geomagnetic field produces several small effects that can be neglected in most satellites. They are also particularly difficult to model for non-symmetric shaped satellites. Below approximately 700 km altitude the drag is the most significant perturbation on orbits, whereas solar radiation pressure is predominant above this altitude and on geo-synchronous orbits (Wertz, 1978). The models presented in this work were implemented in the EDM library to perform disturbance computation on satellites. A manual for EDM usage was produced (Carrara, 2013a) and some results concerning the orbit decay analysis of CBERS satellite was recently published (Kuga et al., 2014). With agreement of the authors of this last reference, the formulation presented here follows the same sequence, except for the gravity gradient and magnetic torque models.

### 2.1 Atmospheric drag modeling

Although a constant drag coefficient is still employed for orbit determination, i.e., for calculating the orbit elements or ephemeris based on satellite position measurements, it has been demonstrated that the interaction of the exosphere molecules with the satellite surface is a complex phenomenon which can be modeled by the kinetic theory of gases, besides some empirical models (Schaaf and Chambré, 1961; Present, 1958; Chapman and Cowling 1970). In order to obtain the aerodynamic force the velocity distribution function of a monomolecular gas in thermal equilibrium and not subjected to a gravitational field has to be used:

$$f = \frac{\rho_o}{m} \left( \frac{m}{2\pi k T} \right)^{3/2} \exp \left[ -\frac{m}{2k T} (\mathbf{v} - \mathbf{v}_o)^2 \right], \quad (1)$$

that gives the probability to find a molecule with velocity between  $\mathbf{v}$  and  $\mathbf{v} + d\mathbf{v}$  with molecular mass  $m$ , in a gas with density  $\rho_o$ , with mean flux velocity  $\mathbf{v}_o$  with respect to a reference frame, and absolute temperature  $T$  ( $k$  is the Boltzmann constant). The velocity distribution function can be employed to compute the momentum transferred by the gas

molecules that strikes a static surface coming from a given direction, as depicted in Fig. 1. To compute the force exerted by the gas on the surface it is assumed (Schaaf and Chambré, 1961) that the momentum exchanged by the molecules both in normal and tangential directions does not depend of the molecule velocity or direction of incidence. A single coefficient seems to be inaccurate to describe the gas surface interaction, and so normal and tangential transfer momentum coefficients were introduced by (Schaaf and Chambré, 1961):

$$\sigma_n = \frac{p_i - p_r}{p_i - p_w}, \text{ and } \sigma_t = \frac{\tau_i - \tau_r}{\tau_i}, \quad (2)$$

that give, respectively, the momentum exchanged in normal and tangential directions.  $p_i$  and  $p_r$  are the momentum carried by the incident and reflected molecules in the surface normal direction, respectively, while  $\tau_i$  and  $\tau_r$  are the momentum in tangential direction of the incident and reflected molecular flux.  $p_w$  stands for the momentum carried out by the reflected molecules in case they arise from the surface with thermal equilibrium with it, at the same surface temperature. For elastic collision both  $\sigma_n$  and  $\sigma_t$  are close to zero, and for a fully interaction, where the reflected molecules are in a Maxwellian equilibrium with null velocity and at same surface temperature, the coefficients tend to unit.

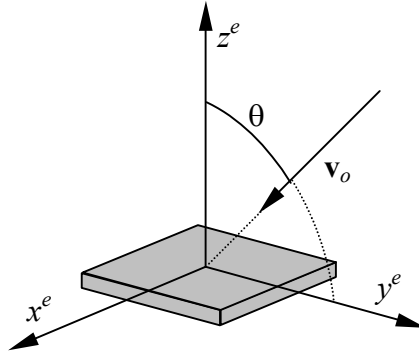


Figure 1. Gas flux hits the surface coming from a known direction.

Now the aerodynamic pressure on a small flat surface can be derived, and results, respectively in normal and incident directions:

$$p_k = -\frac{\rho_i v_o^2}{2} \frac{1}{s^2} \left\{ \left[ \frac{2 - \sigma_n - \sigma_t}{\sqrt{\pi}} s \cos \theta + \frac{\sigma_n}{2} \sqrt{\frac{T_w}{T_i}} \right] \exp(-s^2 \cos^2 \theta) + \left[ (2 - \sigma_n - \sigma_t) s^2 \cos^2 \theta + 1 - \frac{\sigma_n}{2} + \frac{\sigma_n}{2} \sqrt{\pi} \sqrt{\frac{T_w}{T_i}} s \cos \theta \right] [1 + \operatorname{erf}(s \cos \theta)] \right\}, \quad (3)$$

$$p_u = \frac{\rho_i v_o^2}{2} \frac{\sigma_t}{s \sqrt{\pi}} \left\{ \exp(-s^2 \cos^2 \theta) + \sqrt{\pi} s \cos \theta [1 + \operatorname{erf}(s \cos \theta)] \right\}, \quad (4)$$

where  $\rho_i$  is the local atmospheric density,  $T_w$  is the surface absolute temperature,  $T_i$  is the incident flux absolute temperature,  $\operatorname{erf}(\cdot)$  is the error function and  $\theta$  is the incident angle ( $\cos \theta = -\mathbf{n} \cdot \mathbf{u}$ , where  $\mathbf{u}$  is the incident unit vector:  $\mathbf{u} = \mathbf{v}_o / v_o$ ). The speed ratio  $s$  is the ratio between the flux mean velocity,  $\mathbf{v}_o$ , and the most probable velocity of the molecules, given by

$$s = |\mathbf{v}_o| \sqrt{\frac{m}{2k T_i}}. \quad (5)$$

The aerodynamic pressure shall be integrated over the external satellite surface, so as to give the force acting on the satellite:

$$\mathbf{f}_{aer} = \int_{A_{ext}} (p_k \mathbf{n} + p_u \mathbf{u}) dA. \quad (6)$$

The integration shall be performed over all the external satellite surfaces, but care must be taken because only convex shaped satellites are valid. In fact, since the distribution function of the reflected beam differs from the incident flux due to thermal accommodation, double or triple molecule collision with the satellite are not taken into account. Normally this effect can be neglected and the integration error for concave shaped satellites is small. The “shadowing” effect, where a part of the satellite like an antenna or panel occludes another part in the mean flux direction, makes the integral differ from the correct one (Schamberg, 1967). Although the molecules strike the satellite coming from any direction, the main contribution to the force are the ones in the flux direction. For convex satellites with constant surface properties (temperature and momentum coefficients) and simple geometry, like sphere, cylinder, cone and box, the aerodynamic force (and, eventually, also the torque) can be analytically integrated over the external surface (Elliott and Rasmussen, 1969; Sentman and Karamcheti, 1969; Cook, 1960; Stalder and Zurick, 1951; Carrara, 2013b). Unfortunately, experimental data about the momentum transfer coefficients are scarce. They seem to show, however, that the reflection tends to be diffuse ( $\sigma_n$  and  $\sigma_t$  close to unit) even for highly polished surfaces (Schaaf and Chambré, 1961).

The aerodynamic torque is calculated in a similar way, by integrating it over the satellite external surface:

$$\mathbf{g}_{aer} = \int_{A_{ext}} \mathbf{r}_c \times (p_k \mathbf{n} + p_u \mathbf{u}) dA, \quad (7)$$

where  $\mathbf{r}_c$  is the position of the element centroid in body fixed coordinates.

The thermosphere properties can be computed by any empirical model, like the Jacchia-Lineberry (Mueller, 1982) or the Jacchia-77 thermospheric model (Jacchia, 1977), although several other models are available for orbit and attitude simulation (Carrara, 2011a). The thermospheric models depend on the mean and observed Solar Flux at 10.7 cm wavelength at a given date. The flux varies with solar activity, which presents a 10.6 years cycle. During solar storms, the solar wind deflects the geomagnetic field, which causes a significant heating in the thermospheric molecules. This effect is named geomagnetic activity and is measured by geomagnetic observatories spread around the world. Both the solar flux and geomagnetic activity were compiled and stored in a single file, together with the flux mean values necessary to feed the models, and are freely available (Carrara, 2011a).

## 2.2 Solar radiation modeling

The solar radiation force can be modeled in a similar way to that one of the aerodynamic drag. The incidence of Sun light on a satellite produces a force due to the exchange of momentum between the light photons and the surface (Carrara, 2013b; NASA, 1969; Georgevic, 1973). At the Earth distance from Sun, the pressure of the sunlight over a flat plane of 1 square meter is approximately 4.5  $\mu\text{N}$ . The pressure at a distance  $R$  in astronomical units from Sun is computed by

$$p = \frac{S_o}{c} \left( \frac{1}{R} \right)^2, \quad (8)$$

where  $S_o$  is the solar power at 1 astronomical unit distance from Sun ( $S_o = 1353 \text{ W/m}^2$ ), and  $c$  is the light speed. The force on a flat plane is obtained by assuming that the incident beam can be reflected partially in the specular direction, partially scattered by the surface, and partially absorbed or transmitted. Two coefficients are necessary to describe the reflection phenomenon: the specular fraction,  $e$ , and the diffuse fraction,  $\delta$ . If  $\alpha$  is the absorbed and transmitted fraction, the coefficients shall obey  $e + \delta + \alpha = 1$ . The absorbed fraction heats the surface and it emits diffuse radiation according to the Stefan-Boltzmann law:

$$S_i = \varepsilon \sigma T_w^4, \quad (9)$$

where  $S_i$  is the emitted power,  $\varepsilon$  is the surface emissivity,  $\sigma$  is the Stefan-Boltzmann constant ( $\sigma = 5,667 \cdot 10^{-8} \text{ W/m}^2 \text{ K}^4$ ) and  $T_w$  is the surface absolute temperature. By assuming that the reflection model follows the Lambert cosine law, the force components in normal direction,  $\mathbf{n}$ , and incident direction,  $\mathbf{s}$ , can be obtained, resulting

$$p_n = -p \cos \eta \left[ 2e \cos \eta + \frac{2}{3} \delta \right] - \frac{2}{3} \frac{\sigma}{c} \varepsilon T_w^4, \quad (10)$$

$$p_s = p \cos \eta (1 - e), \quad (11)$$

where  $\eta$  is the light incidence angle with respect to the surface normal ( $\cos \eta = -\mathbf{n} \cdot \mathbf{s}$ ). The elementary solar pressure force shall be integrated over the external surface in a similar way to that employed in the aerodynamic force computation:

$$\mathbf{f}_{srp} = \int_{A_{ext}} (p_n \mathbf{n} + p_s \mathbf{s}) dA, \quad (12)$$

and, as before, mutual shadowing shall be avoid in the integration. That excludes, of course, the concave satellites, although the error committed when the shadow is neglected depends on the satellite geometry and is, normally, small. Therefore, only external surfaces that are exposed to the sunlight shall be considered in the integration. They must obey the condition  $\cos \eta > 0$ , otherwise they shall be omitted from computation, except by the emitted parcel. The radiation force can then be expressed as

$$\mathbf{f}_{srp} = \begin{cases} \int_{A_{ext}} (p_n \mathbf{n} + p_s \mathbf{s}) dA, & \text{if } \cos \eta > 0 \\ -\frac{2}{3} \frac{\sigma}{c} \varepsilon \int_{A_{ext}} T_w^4 \mathbf{n} dA, & \text{if } \cos \eta \leq 0 \end{cases}. \quad (13)$$

If the external surface temperature  $T_w$  is constant all over the satellite, then it can be shown that the resultant reemission radiation force is null and can be removed from integration in order to speed up calculations. Although not included in this work, the indirect radiation pressure could easily be implemented, however making the necessary arrangements to integrate over the whole Earth surfaces contributing to the albedo effect (Knocke et alli, 1988). The solar radiation torque  $\mathbf{g}_{srp}$  is computed by integrating the elementary torque on each surface, as in Eq. 7.

## 2.3 Earth's gravitational field

A satellite in a low Earth orbit is submitted to several disturbance effects besides the ones related on previous sections. The Earth gravitational field is far from being uniform, and the subtle variations in the gravitational force makes the orbit trajectory not elliptic as should be.

Any Earth artificial satellite is subject to attraction by the non-central gravitational field and suffers disturbances due to non-spherical and non-symmetrical distribution of Earth mass. The potential of the satellite relative to the unevenly distributed Earth mass is calculated in a generic form by:

$$V = \frac{GM_e}{r} \sum_{n=0}^{\infty} \sum_{m=0}^M \left( \frac{a}{r} \right)^n \left[ \bar{C}_{nm} \cos m\lambda + \bar{S}_{nm} \sin m\lambda \right] \bar{P}_{nm}(\sin\psi), \quad (14)$$

where  $V$  is the potential,  $G$  is the universal gravitational constant,  $M_e$  is the Earth mass,  $M$  is the truncation index,  $r$  is the distance to body from the Earth center,  $a$  is the Earth equatorial radius,  $\lambda$  is the longitude of body,  $\psi$  is the geocentric latitude of body,  $\bar{P}_{nm}$  are the fully normalized Legendre polynomials of order  $n$  and degree  $m$ , and  $\bar{C}_{nm}, \bar{S}_{nm}$  are the fully normalized spherical harmonics coefficients. In this work the standard forward-column implementation proposed by Holmes and Featherstone (2002) to higher order and degree was coded, as described in Kuga and Carrara (2013), which showed its performance in computation of Earth orbits up to order 2159 and degree 2190, corresponding to EGM2008 model. It is preferred to reverse the order of computation of the summation on Eq. 14, where the outer loop in  $m$  is first computed. The summation in the geopotential is then rewritten as:

$$V = \frac{GM}{r} + \frac{GM}{r} \sum_{m=0}^M \left[ \cos(m\lambda) \sum_{n=\mu}^M \left( \frac{a}{r} \right)^n \bar{C}_{nm} \bar{P}_{nm}(\theta) + \sin(m\lambda) \sum_{n=\mu}^M \left( \frac{a}{r} \right)^n \bar{S}_{nm} \bar{P}_{nm}(\theta) \right], \quad (15)$$

where  $0^\circ \leq \theta \leq 180^\circ$  is the co-latitude, and defining the inner summation components by:

$$X_{mC} \equiv \sum_{n=\mu}^M \left( \frac{a}{r} \right)^n \bar{C}_{nm} \bar{P}_{nm}(\theta), \quad X_{mS} \equiv \sum_{n=\mu}^M \left( \frac{a}{r} \right)^n \bar{S}_{nm} \bar{P}_{nm}(\theta), \quad (16)$$

$$\Omega_m \equiv \cos(m\lambda) X_{mC} + \sin(m\lambda) X_{mS}, \quad (17)$$

where  $\mu$  is an integer that depends on  $m$ , the potential yields

$$V = \frac{GM}{r} + \frac{GM}{r} \sum_{m=0}^M \Omega_m. \quad (18)$$

The gradient of the potential is then obtained in terms of spherical coordinates  $\lambda, \theta, r$ , and transformed to Cartesian coordinates. The implementation details can be found in Kuga and Carrara (2013). The codes were tested up to order 2159 and degree 2190 without any noticeable flaw. Numerical degradation near the poles was expected, although up to  $0.000001^\circ$  of proximity to the pole, i.e.  $\pm 89.999999^\circ$  latitude, no problems were reported.

## 2.4 Disturbance models

Among the disturbances found in the space environment is worth to mention the ones whose impact in orbit or attitude is relatively strong. From this point of view the Sun-Moon

gravitational disturbance in the orbit parameters play an important role. Contributing for disturbing the attitude are the Earth's gravity gradient and the magnetic torque, sometimes referred to residual magnetic torque. All these perturbations are described in sequel.

The Sun-Moon perturbation on orbit is modeled by supposing that the effect can be approximated by a point of mass attraction. The acceleration due to point mass effects is modeled by:

$$\ddot{\mathbf{r}}_{pm} = \mu_p \left( \frac{\mathbf{r}_p - \mathbf{r}}{|\mathbf{r}_p - \mathbf{r}|^3} - \frac{\mathbf{r}_p}{|\mathbf{r}_p|^3} \right), \quad (19)$$

where  $\mu_p$  is the gravitational coefficient ( $G M_p$ ) of the perturbing body (Sun or Moon), and  $\mathbf{r}_p$  is the inertial position vector of the perturbing body. The only third perturbing bodies considered are the Sun and the Moon, whose inertial coordinates are obtained analytically, with an accuracy of  $10^{-3}$  degrees for the Sun and  $10^{-2}$  degrees for the Moon.

The gravity gradient torque is caused by differences in the gravitational force or acceleration acting on different parts of the satellite. Since the gravitational force on Earth, according to Newton's law, is inversely proportional to the square of the distance, so small differences occur both in intensity and direction of the gravity acting on each element of mass belonging to the satellite, because some elements are closer or farther from the center of the Earth.

The gravity torque with respect to the satellite center of mass of a mass element  $dm$ , as seen in Figure 2, is given by:

$$\mathbf{g}_g = -\mu \int_M \mathbf{r} \times \frac{(\mathbf{R} + \mathbf{r})}{|\mathbf{R} + \mathbf{r}|^3} dm, \quad (20)$$

where  $\mu = 3.986 \times 10^5 \text{ km}^3/\text{s}^2$  is the Earth's gravitational constant,  $\mathbf{R}$  is the position with respect to the Earth center, and  $\mathbf{r}$  is the position of the mass element in body fixed coordinates.

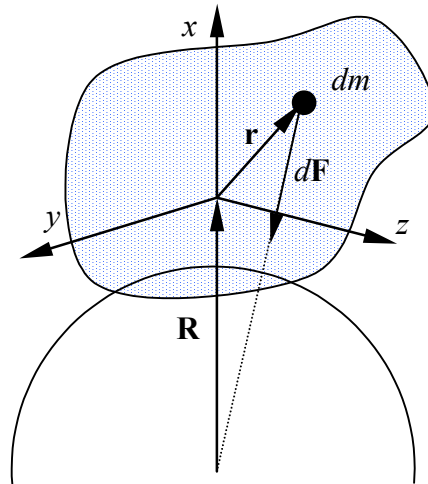


Figure 2. Earth's gravitational force acting on a mass element.

The integral can be evaluated by expanding the gravitational force in power series up to first degree. The gravity gradient torque then results:

$$\mathbf{g}_g = \frac{3\mu}{R^3} \mathbf{v} \times (\mathbf{J} \mathbf{v}), \quad (21)$$

where  $\mathbf{J}$  is the satellite inertia tensor, and  $\mathbf{v}$  is the unit vector of the zenith direction in spacecraft coordinates. Since  $\mathbf{v}$  is the local vertical, the gravity torque is always in the local horizontal plane, which means that the torque drives the satellite smallest principal moment of inertia to be aligned to the local vertical.

The magnetic torque is one of the most perturbing torque on the satellite attitude. It can be generated either by a control action, by means of magnetic torquers (in fact magnetic coils) or by magnetic material and non-compensated electric currents on board. Magnetic torques can arise also by collision of atmospheric ions with the satellite body, which generates electric currents on the surface. Whatever the magnetic source may be, there will be always a magnetic dipole  $\mathbf{m}$  on the satellite. The magnetic dipole is additive, which means that each magnetic or electric source contributes to the overall dipole. If the vector  $\mathbf{m}$  is the resulting (control plus disturbances) magnetic dipole on the satellite, the magnetic torque will be given by:

$$\mathbf{g}_m = \mathbf{m} \times \mathbf{B}, \quad (22)$$

where  $\mathbf{B}$  is the Earth's magnetic field strength in satellite fixed coordinates. Although it is usual to employ magnetic torques for attitude control, it can be noted by Eq. 22 that the torque will always lay in a plane perpendicular to the Earth field so there is no way to generate a 3 axis torque. For accurate pointing requirements a second actuator, usually reaction wheels, are also presented in the satellite.

### 3 THE EDM LIBRARY

In order to establish the technical characteristics for the attitude control of a spacecraft, and to define the sensors and actuators to be employed in a given space mission, usually the designer performs an accurate simulation of the control action subjected to the disturbances encountered in the space environment. The library described here, named Environmental Disturbance Models (EDM), implements several functions to compute the environmental perturbations on both the orbit and attitude of satellites. The updated version of the library includes functions to calculate the aerodynamic forces and torques, solar radiation pressure forces and torques, gravity gradient torque, sun-moon acceleration, magnetic torque and acceleration of the Earth's gravitational field up to order 2159.

The calculation of aerodynamic and solar radiation forces and torques depends on the satellite geometry, which can be described by a boundary-representation, or B-rep, similar to that one employed in computer graphics or finite element theory. The geometry is then described by surfaces defined by mathematical equations or by flat polygons. The representation adopted here was flat polygons, similar to that of OpenGL (Khronos Group, 2014). The satellite external surface is then described by polygons defined by their vertices. Curved surfaces are approximated by subdivisions into small triangles or quads plans. Both the surface normal and area are obtained from the vertex coordinates of a quadrilateral or a triangle element. The aerodynamic and solar pressure forces acting on an area element are then decomposed in the normal  $\mathbf{n}$  and incident ( $\mathbf{v}$  or  $\mathbf{s}$ ) directions, which are known in the spacecraft frame. There are specific functions to set the velocity vector  $\mathbf{v}$  and sun vector  $\mathbf{s}$  to the library. Aerodynamic and solar radiation forces and torques are computed by the functions shown in Figure 3. Figure 4 presents all geometries already implemented in the library. The

functions `edm_aerodynamic_plane`, `edm_aerodynamic_plane_fb` and `edm_solar_prsr_plane` compute the forces on a plane from its normal and surface area. The `edm_aerodynamic_triangle`, `edm_aerodynamic_quad`, `edm_solar_prsr_triangle` and `edm_solar_prsr_quad` functions calculate the normal and area from the vertexes, such that  $\mathbf{n}$  follows the right hand rule of vertexes order supplied to the functions, and then computes the force and torque acting on the element. The `_triangle` functions need 3 vertexes as parameters, while the `_quad` functions accept 4 vertexes. Either computed by the `_plane` or by the `_triangle` or `_quad` functions, it is up to the user to integrate (accumulate) the aerodynamic and radiation pressure over the satellite outer surface. It is emphasized that the integration should be also evaluated over time to enable proper analysis of their effects on the orbit and attitude. For complex geometries the `edm_aerodynamic_mesh` and `edm_solar_prsr_mesh` functions integrate the force and torque from a structure that stores the vertexes, faces and surface properties of the satellite. There are structures to store the vertex table (`vertex`), the triangle table (`mesh`) and the surface properties table (`material`). The mesh table stores also a component identifier that allows easily rotating or translating some parts of the satellite like solar arrays, for instance. Operator functionalities were extended to perform translation, rotation and scaling in the vertex table, based on the component identifier. All these functions are not independent among each other, since the higher level functions, like the `_mesh` function, for instance, use the low-level functions which are based on the area and normal. Functions to compute some previously analytically integrated shapes, like sphere (`edm_aerodynamic_sphere`, `edm_solar_prsr_sphere`), cone (`edm_solar_prsr_cone`), `cylinder` (`edm_aerodynamic_cylinder`, `edm_solar_prsr_cylinder`) and box (`edm_aerodynamic_box`, `edm_solar_prsr_box`) were incorporated to the library to speed up computations, as shown in Figures 3 and 4. However, surface properties like accommodation and reflection coefficients, as well as the surface temperature, is assumed to be constant over the entire shape. They need as input parameter only the shape orientation axis  $\mathbf{i}$ ,  $\mathbf{j}$ ,  $\mathbf{k}$ , with respect to the attitude reference frame. The aerodynamic force on the cone (`edm_aerodynamic_cone`), is performed by numerical integration, since there is no analytical solution for this. There is also the possibility to calculate the forces and torques on a spherical sector (`edm_aerodynamic_sphere_sector`, `edm_solar_prsr_sphere_sector`), with numerical integration (summation) of plane elements defined by longitude and latitude angles. Spherical sectors are usually employed to model antenna dishes. Whatever the function used to compute the forces and torques for a given geometry, it may be combined with any other method, provided all the information necessary for the calculation is given. For example, the aerodynamic forces on a satellite consisting of a quadrilateral panel and a cylinder may be calculated with only two functions: `edm_aerodynamic_cylinder` and `edm_aerodynamic_plane` (or `edm_aerodynamic_quad`).

### 3.1 Geometry description file

Although the functions mentioned above, together with the structures to store the geometry, allow describing the satellite geometry from a program code, it shall be considered that this task can be complex especially if the satellite is composed from a large number of polygons (Ziebart, 2004). A 3D graphical modeling application can then be used to quickly construct the geometry from predefined shapes, and after that this geometry can be exported to the EDM library. Unfortunately many non-commercial 3D modeling applications use binary formats to store the graphic object, which makes the conversion process difficult, if not impossible. A rare exception is Blender (Blender Institute, 2014), which, besides having tools to create and edit complex shapes, performs conversion between different formats, some of

them in plain ASCII. For backward compatibility reasons the EDM library adopted the Nastran (NASA Structure Analysis) format to describe the satellite geometry.

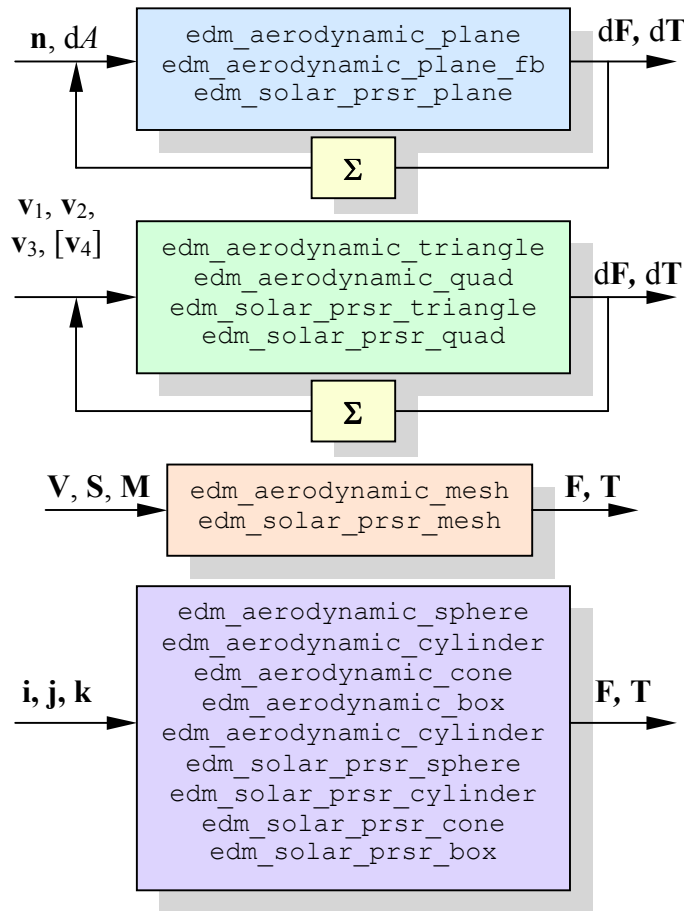


Figure 3. EDM aerodynamic and solar radiation functions to compute forces and torques.

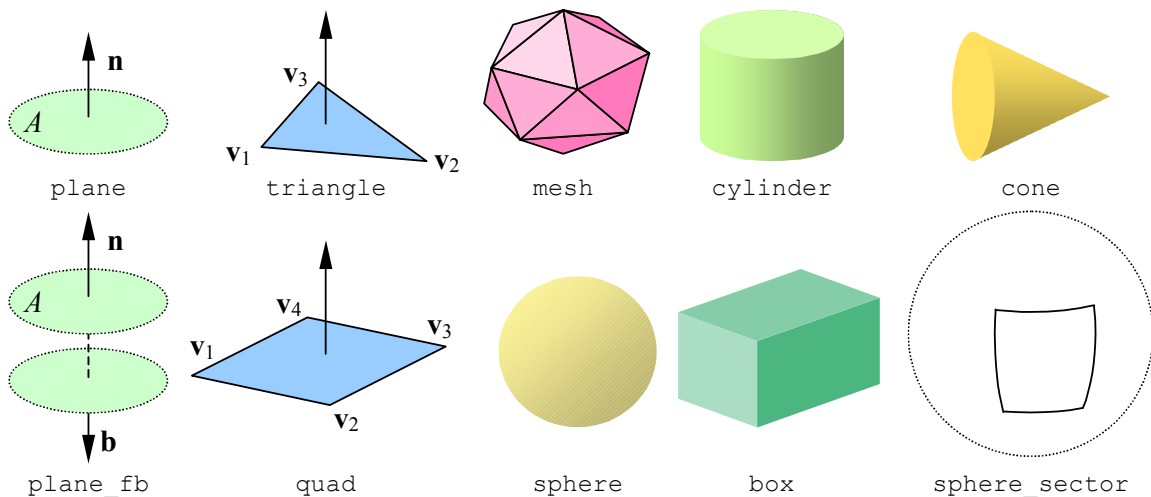


Figure 4. Available geometries of EDM library.

The Nastran uses an ASCII file to store the boundary representation of the geometry in a simple and easy to understand format. The geometry is described by means of vertexes and polygons tables. These tables are identified by an 8-byte command starting on first column of

each record (line) of the file. Only the commands that effectively are used to calculate the forces and torques will be described here. Fortunately, most satellites can be described efficiently with a small number of polygons, which barely reaches 40 triangles. Of course sometimes it is preferable to create the geometry file directly by hand than using a graphic application. It should be taking into account, of course, that small structures such as antennas, brackets, adapters, etc., do not need be included because they do not modify the results significantly. Two new commands were included in the geometry description file, that were not supported by the original Nastran format: MATERIAL and BODYAP. An example of the description file for the China-Brazil Earth Remote Sensing (CBERS) satellite is shown in Table 1.

**Table 1. Geometry description file for satellite CBERS.**

SATID	CBERS						
GRID	1000		0-000.000+1900.00+1100.00				
GRID	1010		0-000.000+8200.00+1100.00				
GRID	1020		0+000.000+8200.00-1100.00				
GRID	1030		0+000.000+1900.00-1100.00				
GRID	1040		0-1000.00+900.000-1100.00				
GRID	1050		0-1000.00+900.000+1100.00				
GRID	1060		0-1000.00-900.000+1100.00				
GRID	1070		0-1000.00-900.000-1100.00				
GRID	1080		0+1000.00+900.000-1100.00				
GRID	1090		0+1000.00+900.000+1100.00				
GRID	1100		0+1000.00-900.000+1100.00				
GRID	1110		0+1000.00-900.000-1100.00				
CQUAD4	1001	1	1000	1010	1020	1030	
CQUAD4	1011	1	1080	1090	1100	1110	
CQUAD4	1021	1	1070	1110	1100	1060	
CQUAD4	1031	1	1050	1090	1080	1040	
CQUAD4	1041	1	1080	1110	1070	1040	
CQUAD4	1051	1	1070	1060	1050	1040	
CQUAD4	1061	1	1060	1100	1090	1050	
BODYAP	1	2	1001	1	200	0	
BODYAP	2	2	1011	0	100	1	
BODYAP	3	2	1021	0	100	1	
BODYAP	4	2	1031	0	100	1	
BODYAP	5	2	1041	0	100	1	
BODYAP	6	2	1051	0	100	1	
BODYAP	7	2	1061	0	100	1	
MATERIAL	100	3	0.90	0.90	0.80	0.00	1.0 350.
MATERIAL	200	3	0.50	0.50	0.50	0.70	0.8 380.
ENDDATA							

The EDM library ignores the command SATID; it's just to remind to whom the geometry belongs to. ENDDATA command signals that the geometry has ended at that point. The vertexes table is given by the GRID commands. The numbers following this command are respectively a unique vertex identification number, the command identification number (0), and the x, y and z coordinates of the vertex, in millimeters. The commands CQUAD4 or CTRIA3 establish the polygon table in terms of a quadrilateral (CQUAD4) or triangles (CTRIA3). The parameters for both are: a unique polygon identification number, the command identification number (1 for both), and the vertex identification number (3 for CTRIA3 and 4 for CQUAD4), following the right hand rule to define the extern normal. The BODYAP command defines the faces of the polygon table that will be used when computing the forces and torques. The remaining polygons will be disregarded. The parameters of BODYAP are the unique face number identification, the command identification number (2), the polygon identification number, the structure part, which means, for instance, if the face belongs to the main body (0) or to a

given movable appendage (starting from 1 up to 8), the material identification number and the face normal definition: 1 means right hand rule for face normal computation, 2 means left hand rule for the normal, and 0 means that both sides will be used when computing the forces. As can be seen in Table 1, the CBERS solar array defined by the first `BODYAP` command belongs to appendage 1 and both sides will be computed, since its last parameter is null. The `MATERIAL` command establishes the surface properties, as mentioned in Sections 2.1 and 2.2. There shall be as many `MATERIAL` commands as needed to define the extern surface properties of the satellite. Its parameters are the unique material identification number, the material command identification number (3), the normal  $\sigma_n$  and tangential  $\sigma_t$  accommodation coefficients, the specular  $e$  and diffuse  $d$  reflection coefficients, the surface emissivity  $\epsilon$ , and the surface absolute temperature  $T_w$  in Kelvin.

The EDM functions `edm_read_vertex`, `edm_read_material` and `edm_read_mesh` read the geometry description file and store the satellite geometry and properties in the structures `vertex`, `material` and `mesh`, respectively. A special function `edm_mesh2pov` writes the geometry and properties in file, which can be used to render a 3D image of the satellite through a POV (POV-Ray, 2013) script program. The script file can be found in Carrara (2013a). Figure 5 presents a view of the CBERS satellite rendered with POV.

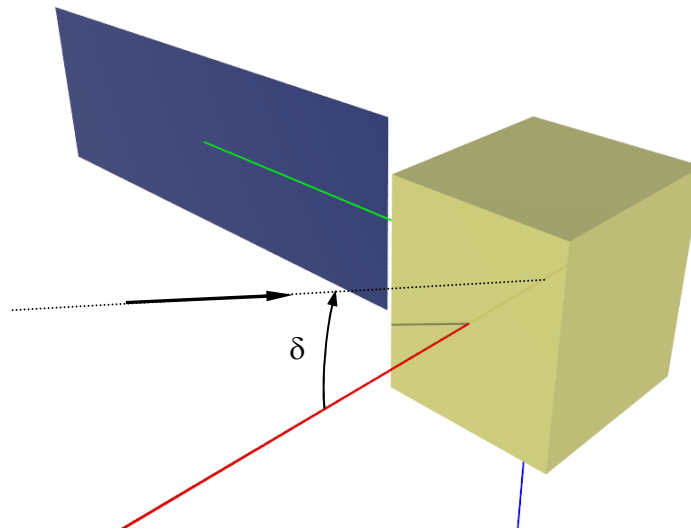


Figure 5. The CBERS satellite geometry rendered with POV-Ray.

Finally, the functions `edm_gravity_gradient`, `edm_magnetic_torque`, `edm_moon_accel`, `edm_sun_accel` and `leg_forcol_ac` compute respectively the Earth's gravity gradient torque, the residual magnetic torque, and the Moon, Sun and Earth gravity acceleration on the satellite.

## 4 EDM EXAMPLES

This section will show some examples of EDM usage. The complete set, as well as the C code can be found on the EDM Manual (Carrara, 2013a). Figure 6 shows the drag coefficient  $C_D$ , defined by

$$C_D = -\frac{2}{\rho_i v_o^2 A_r} \mathbf{f}_{aer} \cdot \mathbf{u} \quad (23)$$

for a cylinder, using numeric integration, where  $A_r$  is the reference area, adopted as  $2LR$  for a cylinder of radius  $R$  and height  $L$ , as function of the incident angle between  $\mathbf{u}$  and the plane perpendicular to the cylinder axes. The cylinder was divided into 180 quadrilaterals (function `edm_aerodynamic_quad`). The curves were compared with the analytical solution of a cylinder (function `edm_aerodynamic_cylinder`) with practically no difference among them.

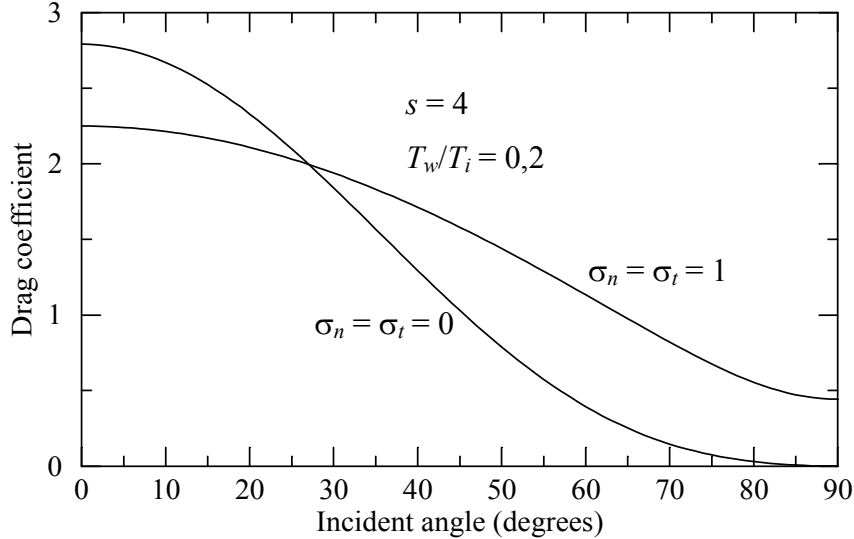


Figure 6. Drag coefficient in a cylinder, as function of the incident angle and the accommodation coefficients.

The radiation pressure force coefficient, computed by

$$C_R = -\frac{\mathbf{f}_{srp} \cdot \mathbf{s}}{p A_r}, \quad (24)$$

is shown in Fig. 7 for a cylinder, as function of the incident angle and the reflection coefficients, for specular, diffuse and no reflection (black body) cases. The curves were obtained with `edm_solar_prsr_cylinder` function.

In the next example the position of the center of pressure of CBERS with respect to the solar radiation pressure will be investigated. The incident angle  $\delta$  is shown in Fig. 5. The center of pressure corresponds to the position  $\mathbf{c}$  in body fixed coordinates where the torque  $\mathbf{g}_{srp}$  is directly generated by the cross product of  $\mathbf{c}$  by the resultant solar pressure force,  $\mathbf{f}_{srp}$ . In other words,  $\mathbf{c}$  is such that:

$$\mathbf{g}_{srp} = \mathbf{c} \times \mathbf{f}_{srp}. \quad (25)$$

However, the force is not always orthogonal to the torque, as does assume the equation. In order to have a solution for Eq. 25, the torque shall be decomposed in a component parallel to the force and other one orthogonal to it, as shown in Figure 8. The orthogonal unit vectors  $\mathbf{u}$ ,  $\mathbf{v}$  and  $\mathbf{w}$  are easily obtained from  $\mathbf{g}_{srp}$  and  $\mathbf{f}_{srp}$ . The torque component along  $\mathbf{u}$  acts as a windmill and does not contribute to the center of pressure. Therefore,  $\mathbf{c}$  must lie on the  $\mathbf{u}$ - $\mathbf{v}$  plane and thus  $\mathbf{c} = c_u \mathbf{u} + c_v \mathbf{v}$ . Again, since  $\mathbf{f}_{srp}$  is in the  $\mathbf{u}$  direction, the  $c_u$  component is undetermined and can be considered null. The center of pressure position then results

$$\mathbf{c} = \frac{\sqrt{\mathbf{f}_{srp}^2 \mathbf{g}_{srp}^2 - (\mathbf{f}_{srp} \cdot \mathbf{g}_{srp})^2}}{\mathbf{f}_{srp}^2} \frac{\mathbf{f}_{srp} \times \mathbf{g}_{srp}}{|\mathbf{f}_{srp} \times \mathbf{g}_{srp}|}. \quad (26)$$

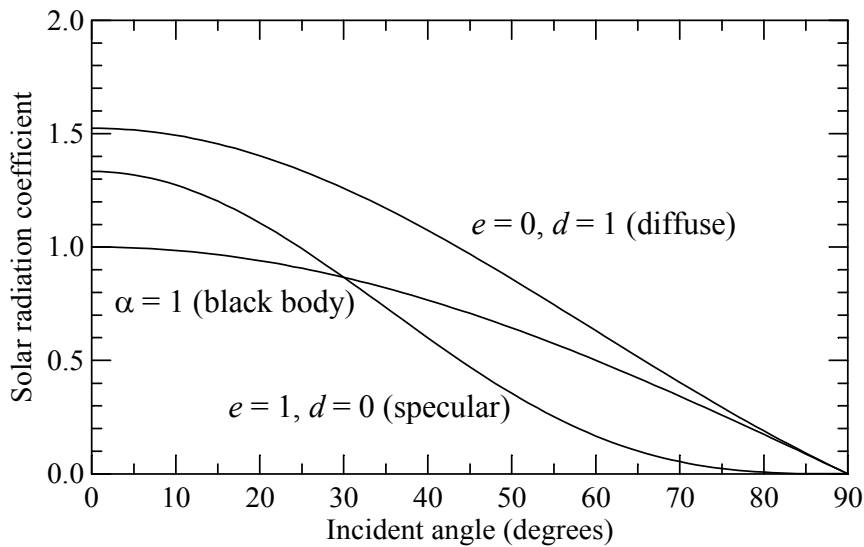


Figure 7. Radiation pressure coefficient for a cylinder as function of the incident angle and reflection coefficients.

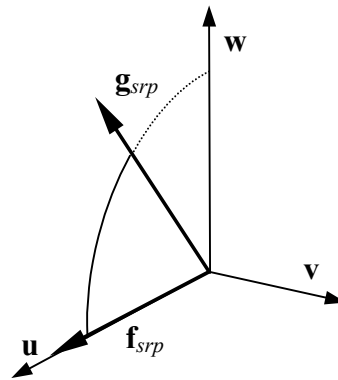


Figure 8. Solar radiation force and torque. The torque lays in plane u-w.

The above expression was calculated for the CBERS as function of the incident angle, using the EDM library. The center of pressure position in the  $x$  and  $z$  directions (respectively the red and blue axis on Fig. 5) resulted null since the satellite is symmetric in the  $y$ -axes. The  $\mathbf{c}$  component in the  $y$  direction due to the solar radiation pressure is presented in Fig. 9. The changing in the center of pressure position is due, mainly, to the projected array area in the incident direction, which decreases as the incident angle deviates from the null position.

The last example is shown in Fig. 10. The objective was to compute the aerodynamic drag and the solar radiation pressure on the CBERS orbit. The drag decreases the orbit semimajor axis along time, and since the mean altitude of the satellite should be constrained within few hundred of kilometers height, maneuvers shall be conducted whenever the orbit reaches its minimum value. The time between maneuvers was around 230 days starting from November 10<sup>th</sup>, 2003. The real orbit, as determined by the CBERS Control Center, is shown in black in Fig. 10. In red it is presented the numerically propagated orbit with aerodynamic and solar radiation forces computed with the EDM library. Both disturbances were computed with the solar array pointing towards the Sun, as it is expected to happen during orbit. The normal and tangential momentum transfer coefficients  $\sigma_n$  and  $\sigma_t$  were adjusted to unit. Although the maximum deviation of the numeric orbit from the estimated orbit was only 60

meters, it is still too large and needs further explanations. Preliminary analysis (Kuga et al., 2014) has shown that the problem probably lays on the daily and the mean solar flux.

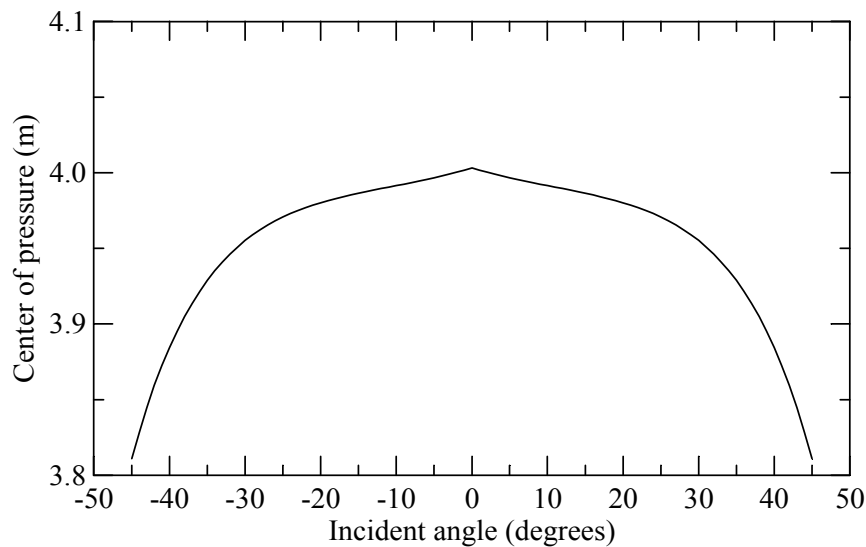


Figure 9. Center of pressure position in the y-axes for CBERS, considering the solar radiation pressure.

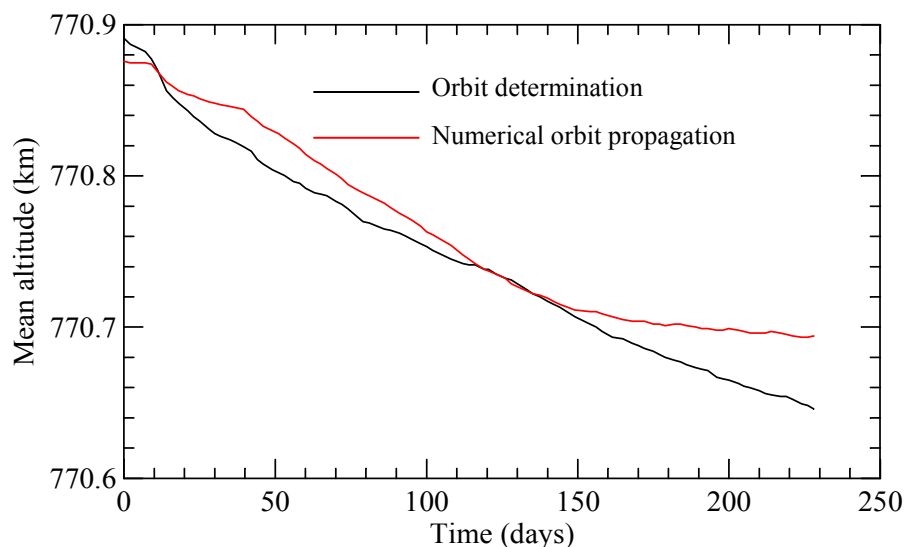


Figure 10. CBERS mean altitude as computed by orbit determination and by numerical propagation including aerodynamic and solar radiation pressure (Source: Kuga et al. 2014).

## 5 CONCLUSIONS

This paper presented the design and development of the EDM library written in C++ with functions to calculate the main disturbances encountered by low Earth orbit satellites in the space environment. This library will be incorporated into an attitude simulator (Carrara, 2011b), which will be used for testing and qualification process of the onboard attitude control software for the Brazilian space missions.

The satellite geometry is described by means of polygons, similar to OpenGL, which allows the generation of complex geometries directly in the program code, or via an ASCII file based on the Nastran geometric description. The library counts also with functions to

calculate the forces and torques in geometries previously integrated such as spheres, cones, cylinders and boxes. It is worth to mention the possibility of making transformations on the geometries, such as rotation, translation or scaling on the satellite as a whole or only part of it, allowing, for example, to perform disturbance analysis when the solar array is rotated to point toward Sun.

Some examples of library usage were presented, in which the drag coefficients and radiation pressure in cylinders were obtained. The analytical expressions for these calculations can be found in Carrara, 2013b. Other example shows the calculation of the center of pressure for the CBERS satellite, considering the solar radiation pressure. Finally, the orbital decay of CBERS was calculated by EDM and compared with the orbit elements measured by the CBERS Control Center. The results showed that there are still some issues to be solved, since the difference was greater than expected.

EDM library was tested with results calculated by other methods (analytical solutions, for instance), and also with results found in the bibliography. Although coding errors can not be disregarded, it is believed that the errors, if any, were minimized during function testing.

## ACKNOWLEDGEMENTS

The author wish to thank the INPE's Satellite Control Center (CCS) that provided the CBERS orbital data.

## REFERENCES

- Blender Institute Blender 3D. Blender Foundation. Available at <http://www.blender.org>. Access in June, 2014.
- Carrara, V. A (Huge) Collection of Interchangeable Empirical Models to Compute the Thermosphere Density, Temperature and Composition. INPE-DMC, Available at <http://www2.dem.inpe.br/val/atmod/default.html>, 2011a.
- Carrara, V. Attitude Simulation Software to Support Brazilian Space Missions. 22nd International Symposium on Space Flight Dynamics. Proceedings. São José dos Campos, Feb-March 2011b.
- Carrara, V. Environmental Disturbance Models (EDM) – User Manual (in portuguese). São José dos Campos: INPE, 2013a. 102 p. (sid.inpe.br/mtc-m19/2013/03.20.14.03-MAN). <http://urlib.net/8JMKD3MGP7W/3DP8Q6B>.
- Carrara, V. Satellite perturbation models (in portuguese). São José dos Campos: INPE, 2013b. 120 p. (sid.inpe.br/mtc-m19/2013/01.23.13.32-PUD). <http://urlib.net/8JMKD3MGP7W/3DE5SHE>.
- Chapman, S.; Cowling, T. G. The mathematical theory of Non-Uniform Gases. 3. ed. Cambridge University Press, UK, 1970.
- Cook, G. E. The Aerodynamic Drag of Near Earth Satellites. London: Her Majesty's Stationary Office, 1960. C.P. No. 523.
- Elliott, J. P.; ; Rasmussen, M. L. Free-molecule Flow past a Cone. AIAA Journal, Vol. 7, No. 1, 1969. pp. 78-86. doi: 10.2514/3.5038.
- Georgevic, R. M. The solar radiation pressure force and torque model. The Journal of the Astronautical Sciences, Vol. 20 No. 5, 1973. pp. 257-274.

- Holmes, S.A.; Featherstone, W.E. A unified approach to the Clenshaw summation and the recursive computation of very high degree and order normalised associated Legendre functions. *Journal of Geodesy*, 76, p. 279-299, 2002.
- Jacchia, L. G. *Thermospheric Temperature, Density and Composition: New Models*. Cambridge, Ma, SAO, 1977. (SAO Special Report No 375).
- Khronos Group. *OpenGL – The Industry’s Foundation for High Performance Graphics*. Beaverton, 2014. Available at: <http://www.opengl.org>. Access in July, 2014.
- Knocke, P. C.; Ries J. C.; Tapley, B. D. Earth Radiation Pressure Effects on Satellites, *Proceedings of the AIAA/ASS Astrodynamics Conference*, (Washington, DC), AIAA Paper 88-4292, 1988. (doi: 10.2514/6.1988-4292).
- Kuga, H. K.; Carrara, V. Fortran- and C-codes for higher order and degree geopotential and derivatives computation. *Proceedings of XVI SBSR - Brazilian Symposium on Remote Sensing*, Iguassu Falls, Brazil, April 13-18, 2013, pp. 2201-2210. <[www.dem.inpe.br/~hkk/software/high\\_geopot.htm](http://www.dem.inpe.br/~hkk/software/high_geopot.htm)>.
- Kuga, H. K.; Carrara, V.; Gagg Filho, L. A. An Improved Drag Model for CBERS Orbit Determination and Propagation. *24th International Symposium on Space Flight Dynamics (ISSFD)*. Laurel, MD, 5-9 May 2014. Available at <https://dnnpro.outer.jhuapl.edu/issfd2014/Agenda.aspx>.
- Mueller, A. C. *Jacchia-Lineberry upper atmosphere density model*. Huston NASA, 1982. (NASA-CR-167824).
- NASA. *Spacecraft Radiation Torques*. NASA Space Vehicle Design Criteria (Guidance and Control). NASA SP-8027, 1969.
- POV-Ray. *The Persistence of Vision Raytracer*. Available at: <http://www.povray.org/>, 2013.
- Present, R. D. *Kinetic Theory of Gases*. McGraw Hill, NY, 1958.
- Schaaf, S. A.; Chambré, P. L. *Fundamentals of gas dynamics - high speed aerodynamics and jet propulsion*. Vol III - Flow of rarefied gases. Princeton, Princeton University Press, 1961. (Princeton Aeronautical Paperbacks, 8).
- Schamberg, R. *On Concave Bodies in Free Molecule Flow*. Rand Corporation, P-3164-1, 1967.
- Sentman, L. H.; Karamcheti, K. Rarefied flow past a sphere. *AIAA Journal*, Vol. 7, No. 1, 1969. pp. 161-163. doi: 10.2514/3.5057.
- Stalder, J. R.; Zurick, V. J. *Theoretical aerodynamic characteristics of bodies in a free-molecule-flow field*. Washington, NACA, 1951. NACA Technical Note 2423.
- Wertz, J. R. *Spacecraft attitude determination and control*. D. Reidel Publishing, 1978.
- Ziebart, M. Generalized analytical solar radiation pressure modeling algorithm for spacecraft of complex shape. *Journal of Spacecraft and Rockets*, 41 (5), pp. 840-848, 2004.